Mirror-assisted tomographic diffractive microscopy with isotropic resolution

E. Mudry, P. C. Chaumet,* K. Belkebir, G. Maire, and A. Sentenac

Institut Fresnel (CNRS UMR 6133), Aix-Marseille Université, Campus de St Jérôme, 13013 Marseille, France
**Corresponding author: patrick.chaumet@fresnel.fr*

Received February 12, 2010; revised April 12, 2010; accepted April 28, 2010;
posted May 7, 2010 (Doc. ID 124244); published May 25, 2010

We demonstrate that the axial resolution of a reflection tomographic diffractive microscope is drastically improved when the sample is placed in front of a perfect mirror. We show analytically and with rigorous simulations that this approach permits us to obtain images with the same isotropic resolution as that obtained when the sample is illuminated and observed from every possible angle. The main difficulty lies in accounting properly for the mirror in the inversion algorithm. © 2010 Optical Society of America

OCIS codes: 180.6900, 110.1758.

Tomographic diffractive microscopy (TDM) is a recent, increasingly used imaging technique that is capable of mapping the three-dimensional (3D) permittivity of label-free samples with high resolution [1–5]. It consists in recording multiple holograms of the sample under various angles of illumination and reconstructing numerically the permittivity map from this set of data. TDM setups are often implemented in conventional high-NA microscopes [1–3,6,7] so that the illumination and the light detection is performed on one side of the sample only. Because of this dissymmetry, the axial resolution of TDM is much poorer than the transverse resolution. The lack of angular coverage imposed by the microscope axial dissymmetry can be partially compensated by rotating the sample [8–10] or by imposing the positivity of the sought dielectric contrast in the inversion procedure [6]. However, these approaches are limited to certain types of samples, and the image resolution remains generally below that which would be obtained with a complete isotropic tomography configuration where the sample is illuminated and observed from every possible angle. In this Letter, we show that placing the sample in front of a mirror in a standard reflection TDM configuration permits us to compensate entirely the dissymmetry of the setup. The main difficulty is in separating the top and bottom views of the sample from the diffracted far field. We show that this task, which is quite complex in the "simplified" two-dimensional (2D) scalar case [11–13] becomes relatively easy in the 3D vectorial configuration. Rigorous simulations of transmission, reflection, and mirror-assisted reflection TDM experiments support our analytic demonstration.

We first briefly sketch the principles of TDM in free space. Let us consider a sample in vacuum, described by its relative permittivity $\epsilon(\mathbf{r})$. The sample is illuminated by a monochromatic incident field $\mathbf{E}^{\mathrm{ref}}$, which is assumed to be a plane wave with wave vector $\mathbf{k}^{\mathrm{inc}}$, $k^{\mathrm{inc}} = 2\pi/\lambda = k_0 : \mathbf{E}^{\mathrm{ref}} = \mathbf{E}^0 e^{i\mathbf{k}^{\mathrm{inc}}.\mathbf{r}}$. We detect in far field $\mathbf{E}^{\mathrm{d}}$, the field diffracted along the $\mathbf{k}$ direction at the position $\mathbf{R}$. Under the renormalized Born approximation [14], one obtains

$$\mathbf{E}^{\mathrm{d}}(\mathbf{k}) = \int \overleftrightarrow{\mathcal{G}}(\mathbf{k},\mathbf{r})\alpha(\mathbf{r})\mathbf{E}^{\mathrm{ref}}(\mathbf{r})\mathrm{d}\mathbf{r}, \tag{1}$$

where $\alpha(\mathbf{r}) = \frac{3}{4\pi}[\epsilon(\mathbf{r}) - 1]/[\epsilon(\mathbf{r}) + 2]$ is the density of polarizability of the object and $\mathcal{G}(\mathbf{k},\mathbf{r})\mathbf{p}$ is the vectorial electric field in the $\mathbf{k}$ direction radiated by a dipole $\mathbf{p}$ placed at $\mathbf{r}$. Because, in free space, [15] $\overleftrightarrow{\mathcal{G}}(\mathbf{k},\mathbf{r})\mathbf{p} = \frac{e^{ik_0R}}{R}e^{-i\mathbf{k}.\mathbf{r}}\mathbf{k}\times(\mathbf{k}\times\mathbf{p})$, one obtains

$$\mathbf{E}^{\mathrm{d}}(\mathbf{k}) = \frac{e^{ik_0R}}{R}\tilde{\alpha}(\mathbf{k}-\mathbf{k}^{\mathrm{inc}})[\mathbf{k}\times(\mathbf{k}\times\mathbf{E}^0)], \tag{2}$$

where $\tilde{\alpha}(\mathbf{k}-\mathbf{k}^{\mathrm{inc}})$ is the 3D Fourier transform of the polarizability. Hence, there is a one-to-one correspondence between the measured scattered field and the spatial frequency of the permittivity. By varying the incident and observation angles, one covers a 3D Fourier domain over which $\tilde{\epsilon}$ is known. The larger this domain, the better the resolution. In the complete configuration [see Fig. 1(c)], if one assumes an infinite signal-to-noise ratio, the accessible Fourier domain is a sphere with radius $2k_0$ [7]. The point-spread function (PSF) of the imager, F, will be given by the inverse Fourier transform of the low-pass filter, which is equal to 1 in the accessible Fourier domain and 0 elsewhere. In the complete configuration, where the sample is illuminated and observed from every possible angles, F is isotropic:

$$F^{\mathrm{iso}}(r) = \frac{1}{2\pi^2 r^3}[\sin(2k_0r) - 2k_0r\cos(2k_0r)]. \tag{3}$$

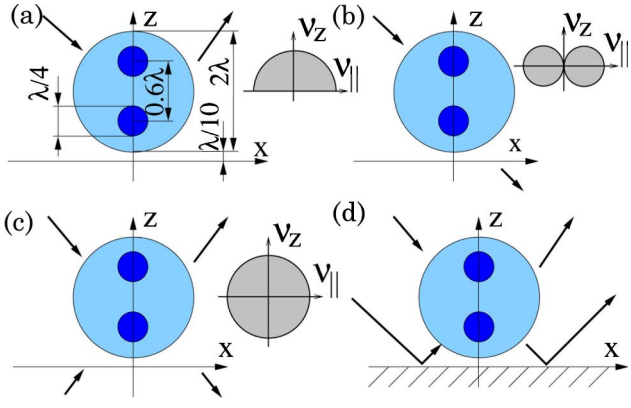

Fig. 1. (Color online) Description of different TDM configurations (insets, accessible Fourier domain). (a) Reflection (half-sphere of radius $2k_0$). (b) Transmission (tore with circular section of radius k_0). (c) Isotropic (sphere of radius $2k_0$). (d) Mirror-assisted reflection configuration (sphere of radius $2k_0$).

 © 2010 Optical Society of America

The resolution, which corresponds to the Rayleigh criterion, is given by the first zero of F. It is about 0.35λ. For TDM setups based on reflection or transmission microscopes [Figs. 1(a) and 1(b)], the accessible Fourier domain of the sample permittivity is only a portion of the $2k_0$ sphere. We plot in Fig. 2 the PSF of a transmission and reflection TDM configuration (with NA = 1). The PSF of the transmission TDM is real and strongly elongated along the z axis. The PSF of the reflection configuration is complex. If the sample is a pure phase object, the resolution of the real part of the reconstructed permittivity is isotropic and similar to that of the complete configuration. However, if the object is absorbing and dephasing light, the real and imaginary parts of the reconstructed permittivity mingle in an unpredictable way.

We now turn to the study of a reflection TDM setup in which the sample is placed in front of a mirror, as shown in Fig. 1(d). In this case, the field diffracted by the sample in the $\mathbf{k}$ direction is given by Eq. (1), where $\mathbf{E}^{\mathrm{ref}}$ is the field that would exist without the sample (i.e., the incident plus the reflected field) and $\mathcal{G}(\mathbf{k},\mathbf{r})\mathbf{p}$ is the field radiated by a dipole $\mathbf{p}$ in the presence of a mirror. For simplicity, we assume that the mirror is placed at $z=0$. If the mirror is perfect, the field radiated by the dipole $\mathbf{p}$ at $(\mathbf{r}_\parallel, z)$ above the mirror is equal to the field radiated by two dipoles $\mathbf{p}=\mathbf{p}_\parallel + p_z\hat{\mathbf{z}}$ at $(\mathbf{r}_\parallel, z)$ and $\mathbf{p}'=-\mathbf{p}_\parallel + p_z\hat{\mathbf{z}}$ at $(\mathbf{r}_\parallel, -z)$ in free space.

Noting $\tilde{\tilde{\alpha}}$ as the cosine transform along the z axis of the 2D Fourier transform along the x and y axes of the polarizability density,

$$\tilde{\tilde{\alpha}}(k_z,\mathbf{k}_\parallel)=\int \mathrm{d}\mathbf{r}_\parallel \int_0^\infty \alpha(\mathbf{r})\cos(k_z z)\exp(-i\mathbf{k}_\parallel.\mathbf{r}_\parallel)\mathrm{d}z, \quad (4)$$

the diffracted field can be written as

$$\mathbf{E}^{\mathrm{d}}(\mathbf{k})=\frac{e^{ik_0R}}{R}(\mathbf{A}f^- + \mathbf{B}f^+), \quad (5)$$

$$f^\pm=\tilde{\tilde{\alpha}}(k_z+k_z^{\mathrm{inc}},\mathbf{k}_\parallel-\mathbf{k}_\parallel^{\mathrm{inc}}) \pm \tilde{\tilde{\alpha}}(k_z-k_z^{\mathrm{inc}},\mathbf{k}_\parallel-\mathbf{k}_\parallel^{\mathrm{inc}}), \quad (6)$$

$$\mathbf{A}=\mathbf{k}\times(\mathbf{k}\times\mathbf{E}_\parallel^0), \qquad \mathbf{B}=E_z^0\mathbf{k}\times(\mathbf{k}\times\hat{\mathbf{z}}). \quad (7)$$

Hence, contrary to the free-space configuration, the scattered field is now related to two cosine-Fourier coefficients of the polarizability [11]. When the incident field satisfies $E_z^0 \neq 0$, the two cosine-Fourier coefficients are easily deduced from the measure of two components of the diffracted field (provided $\mathbf{A}$ and $\mathbf{B}$ are not collinear). Varying $\mathbf{k}^{\mathrm{inc}}$ and $\mathbf{k}$ in 2π sr yields $\tilde{\tilde{\alpha}}(\nu_z,\boldsymbol{\nu}_\parallel)$ for all $\boldsymbol{\nu}$, satisfying $\nu<2k_0$, $\nu_z>0$. When s-polarized incident light is used, $E_z^0=0$. The retrieval of $\tilde{\tilde{\alpha}}(\nu_z,\boldsymbol{\nu}_\parallel)$ is more difficult but still possible. Indeed, for any reachable $\boldsymbol{\nu}$, we can find $\mathbf{k}$ and $\mathbf{k}^{\mathrm{inc}}$ such that $(k_z+k_z^{\mathrm{inc}},\mathbf{k}_\parallel-\mathbf{k}_\parallel^{\mathrm{inc}})=(0,\boldsymbol{\nu}_\parallel)$ and $(k_z-k_z^{\mathrm{inc}},\mathbf{k}_\parallel-\mathbf{k}_\parallel^{\mathrm{inc}})=(\nu_z,\boldsymbol{\nu}_\parallel)$. Measuring one component of the diffracted field for these specific incident and diffracted angles yield $\tilde{\tilde{\alpha}}(0,\boldsymbol{\nu}_\parallel)-\tilde{\tilde{\alpha}}(\nu_z,\boldsymbol{\nu}_\parallel)$. Performing an inverse cosine-Fourier transform of the latter permits retrieval of the polarizability of the sample plus an unwanted Dirac contribution on the $z=0$ plane, which can be easily discarded. Note that both methods necessitate out-of-plane measurements. If only in-plane measurements are performed (as in 2D configurations), the separation of the two coefficients requires sending two cross-polarized sets of incident light.

Once $\tilde{\tilde{\alpha}}$ is retrieved from the scattered field, one can reconstruct α (and the permittivity) by simply performing a one-dimensional cosine transform in the z direction and a 2D Fourier transform in the transverse plane. If a pointlike object is placed at $(0,0,h)$ above the mirror, its reconstructed image (or PSF) will be

$$F^{\mathrm{mirror}}(\mathbf{r}_\parallel,z,h)=F^{\mathrm{iso}}\left(\sqrt{r_\parallel^2+(z-h)^2}\right)+F^{\mathrm{iso}}\left(\sqrt{r_\parallel^2+(z+h)^2}\right). \quad (8)$$

Note that the PSF is no longer a convolution operator. Yet, if the object is placed at one wavelength above the mirror, the second term on the right-hand side becomes negligible and one retrieves the isotropic PSF of the complete configuration.

To illustrate our analysis, we simulate a TDM experiment under transmission, reflection, and mirror-assisted reflection configurations. The sample is a lossless dielectric sphere ($\epsilon=1.01$) containing two absorbing spherical inclusions with permittivity $\epsilon=1.01+0.02i$, as depicted in Fig. 1(a). The far field diffracted by the sample placed in free space or on a mirror is calculated rigorously and corrupted with noise-to-signal ratio of 5% [14,16]. The incident (respectively, diffracted) waves are sent (respectively, detected) in a cone, with half-angle 70° corresponding to NA = 0.95. We use 64 incident plane waves and 121 observation directions regularly spaced within the incident and observation cones. All the incident plane waves are s-polarized so that only one component of the diffracted field needs to be measured (which simplifies greatly the experimental setup). To retrieve the permittivity map from the diffracted far field, one uses a reconstruction procedure based on a conjugate gradient algorithm with a scattering model assuming Born's approximation [14]. This iterative technique accounts easily for the redundancy or lack of data and permits skipping the retrieval of $\tilde{\tilde{\alpha}}$ from the data in the mirror-assisted case. Note that our algorithm has been tested efficiently against real data [17]. Figure 3 displays the real and

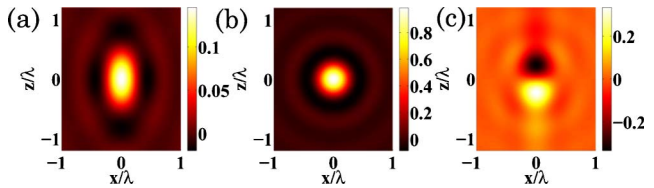

Fig. 2. (Color online) PSFs of the different TDM configurations represented in Fig. 1 (NA is equal to 1 in all cases). (a) Transmission. (b) Complete isotropic configuration. This plot also represents the real part of the PSF in the reflection configuration and the PSF of the mirror-assisted reflection configuration if the pointlike object is placed at one wavelength, at least, above the mirror. (c) Imaginary part of the PSF of the reflection configuration.

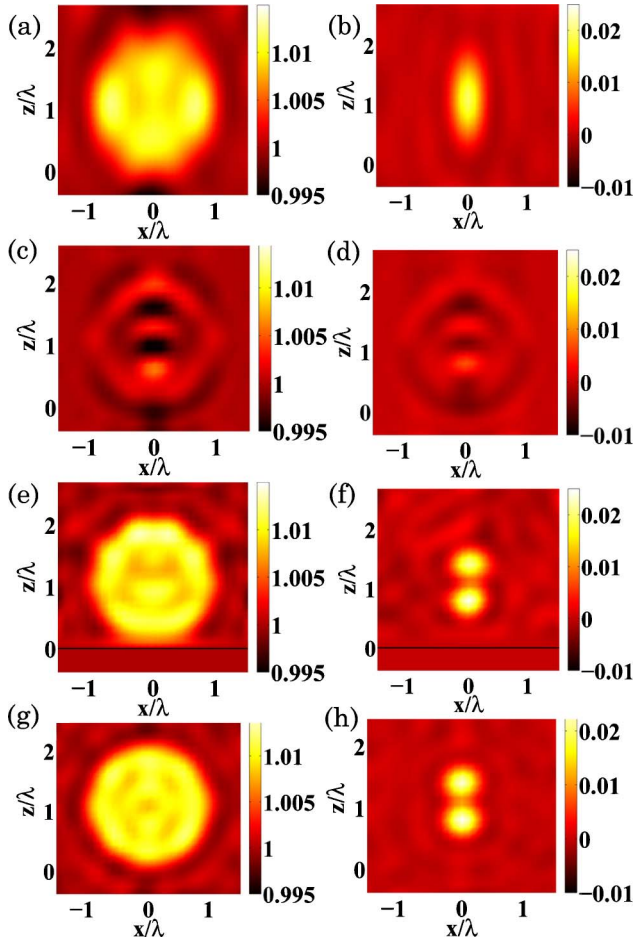

Fig. 3. (Color online) Real and imaginary parts of the reconstructed permittivity for (a) and (b) transmission setup, (c) and (d) reflection setup, and (e) and (f) mirror setup (the sample is placed at $\lambda/10$ above the mirror), (g) and (h) complete free-space configuration.

imaginary parts of the reconstructed permittivity obtained for the different configurations.

The transmission configuration is not able to distinguish the two inclusions owing to its poor axial resolution. The reflection configuration yields strongly distorted images, because it mixes the real and imaginary parts of the permittivity. On the other hand, the mirror-assisted reflection configuration gives reconstructions that are similar to those obtained with a complete tomography configuration [Figs. 3(g) and 3(h)]. The dielectric sphere and the two absorbing inclusions are retrieved with the accurate optogeometric values. Note that the object is placed close to the mirror, i.e., in a region where the global illumination $\langle I \rangle$, which is obtained by averaging over the incident angles the intensity of the stationary pattern created by the incident and reflected waves, $\langle I \rangle \propto 1 - J_0(2k_0 z)$, is the most inhomogeneous. We have performed several imaging experiments with the same object moved away from the mirror by steps of $\lambda/10$ and obtained similar reconstructions. Of course, neglecting the mirror in the inversion procedure yielded totally distorted and striped reconstructions.

In conclusion, mirror-assisted reflection optical diffraction tomography seems to be an efficient solution for imaging label-free samples with high isotropic resolution. The experimental implementation is similar to that of standard reflection TDM, except that the sample is placed in the vicinity of a mirror. The important point is to account for the mirror in the inversion procedure.

References

1. V. Lauer, J. Microsc. **205**, 165 (2002).
2. W. Choi, C. Fang-Yen, K. Badizadegan, S. Oh, N. Lue, R. R. Dasari, and M. S. Feld, Nat. Meth. **4**, 717 (2007).
3. M. Debailleul, V. Georges, B. Simon, R. Morin, and O. Haeberlé, Opt. Lett. **34**, 79 (2009).
4. S. A. Alexandrov, T. R. Hillman, T. Gutzler, and D. D. Sampson, Phys. Rev. Lett. **97**, 168102 (2006).
5. G. Maire, F. Drsek, J. Girard, H. Giovannini, A. Talneau, D. Konan, K. Belkebir, P. C. Chaumet, and A. Sentenac, Phys. Rev. Lett. **102**, 213905 (2009).
6. Y. Sung, W. Choi, C. Fang-Yen, K. B. zadegan, R. R. Dasari, and M. S. Feld, Opt. Express **17**, 266 (2009).
7. R. Fiolka, K. Wicker, R. Heintzmann, and A. Stemmer, Opt. Express **17**, 12407 (2009).
8. F. Charrière, N. Pavillon, T. Colomb, C. Depeursinge, T. J. Heger, E. A. D. Mitchell, P. Marquet, and B. Rappaz, Opt. Express **14**, 7005 (2006).
9. S. S. Kou and C. J. R. Sheppard, Opt. Lett. **33**, 2362 (2008).
10. S. Vertu, J.-J. Delaunay, I. Yamada, and O. Haeberlé, Cent. Eur. J. Phys. **7**, 22 (2009).
11. F. Natterer, Wave Motion **45**, 776 (2008).
12. C. J. Nolan, M. Cheney, T. Dowling, and R. Gaburro, Inverse Probl. **22**, 1817 (2006).
13. A. J. Devaney, J. Opt. Soc. Am. A **21**, 2216 (2004).
14. K. Belkebir, P. C. Chaumet, and A. Sentenac, J. Opt. Soc. Am. A **22**, 1889 (2005).
15. J. D. Jackson, *Classical Electrodynamics*, 2nd ed. (Wiley, 1975).
16. P. C. Chaumet, K. Belkebir, and A. Sentenac, Opt. Lett. **29**, 2740 (2004).
17. P. C. Chaumet, K. Belkebir, and A. Sentenac, J. Appl. Phys. **106**, 034901 (2009).